

Sonographic Morphology of Infiltrating Breast Carcinoma

Relationship With the Shape of the Hyaluronan Extracellular Matrix

Philippe Vignal, MD, Marie Reine Meslet, MD,
Jean Michel Roméo, MD, Franck Feuilhade, MD, PhD

Objective. To compare the shape of the sonographic image of invasive breast cancer with the shape of the corresponding histopathologic section stained for components of the extracellular matrix, hyaluronan, and collagen. **Methods.** We studied 22 cases of breast carcinoma. Among them, 13 were visible on both sonography and mammography, whereas 9 were visible only on sonography. We compared the sonographic images with the histologic sections of the same carcinomas after staining with alcian blue for hyaluronan and Masson trichrome for collagen. **Results.** We have shown that the shape of the sonographic image of breast cancer is similar to the shape of its hyaluronan extracellular matrix. **Conclusions.** This finding explains why breast sonography is so sensitive for detection of invasive carcinoma and why some invasive cancers are not visible on mammography. **Key words:** breast sonography; mammography; breast cancer; extracellular matrix; hyaluronan; collagen.

It is well established that sonography is a very accurate technique for assessing the size of breast cancer,^{1,2} but, to our knowledge, the relationship between invasive breast cancer echo morphology and histopathologic characteristics has not been investigated in detail. Because a substantial part of the tumor's volume is made up of a hyaluronan extracellular matrix,³⁻⁵ we sought to compare the shape of the sonographic image on invasive breast cancer with the shape of the corresponding histopathologic section stained for hyaluronan and collagen, the main components of the extracellular matrix.

Materials and Methods

In this retrospective study, breast sonography was performed in 22 consecutive patients (mean age, 52 years) with pathologically proven invasive ductal carcinoma who were referred to a breast sonographic specialist. Between 1995 and 1997, the same operator (P.V.) using a

Received November 1, 2001, from Unité de Sénologie, Centre Hospitalier Universitaire Henri Mondor, Créteil, France. Revision requested November 29, 2001. Revised manuscript accepted for publication December 19, 2001.

We thank Philippe Coquel, MD, for reviewing the manuscript.

Address correspondence and reprint requests to Philippe Vignal, MD, 33 rue Nicolo, 75116 Paris, France.

Toshiba SSD-250 system (Toshiba Medical Systems Co, Ltd, Tokyo, Japan) performed the sonographic examinations with a 7.5-MHz linear array transducer. These 22 cases of invasive ductal carcinoma comprised consecutive cases independent of sonographic or mammographic findings. All patients were informed orally and gave their consent to this protocol.

The mean tumor diameter was 13 mm, palpable in 8 (36%) of 22 cases. Figure 1 shows the size range of the lesions. Mammograms were obtained in all cases and showed negative findings in 9. In these 9 cases, the sonographic examinations were performed because of mammographically dense breasts (n = 8) or a palpable mass (n = 1). The diagnosis was obtained by fine-needle aspiration cytologic examination under sonographic guidance. Dense breasts were found in 18 (82%) of 22 patients. Among them, 13 (59%) were taking hormone replacement treatments.

The following elements of the sonographic pattern were recorded: the shape of the lacuna, margins, posterior shadowing, and the internal echo pattern. We were not aware of outcomes and pathologic results before describing the sonograms. In addition, 2 adenofibromas were studied as well as an ex vivo umbilical cord.

The sonographic scans and pathologic sections were made through the greatest diameter of the tumor. Four-micrometer-thick sections were cut, embedded in paraffin blocks, and stored in the same pathology laboratory. Initial staining with hematoxylin-eosin was made to confirm the presence of tumor. To show glycosaminoglycan, the usual alcian blue stain, specific for hyaluronic acid, was used at pH 2.5; alcian blue stains blue

on a pink background. Collagen fibers were stained blue with Masson trichrome. The adipose tissue was clearly identified without any staining.

The glass histologic slides and sonographic scans were compared on a 1/1 scale by manual superimposition. This enabled positioning of the skin surface. The slides were then displayed on a computer screen at $\times 20$ magnification. At this magnification, the different components of the tumors were clearly visible. For production of the screen display, the glass slides were digitized on a backlit scanner. The slides were laid directly on the scanner before magnification and optimization by modifying contrast and luminosity. Printouts were produced for precise study of the different components inside and outside the tumor.

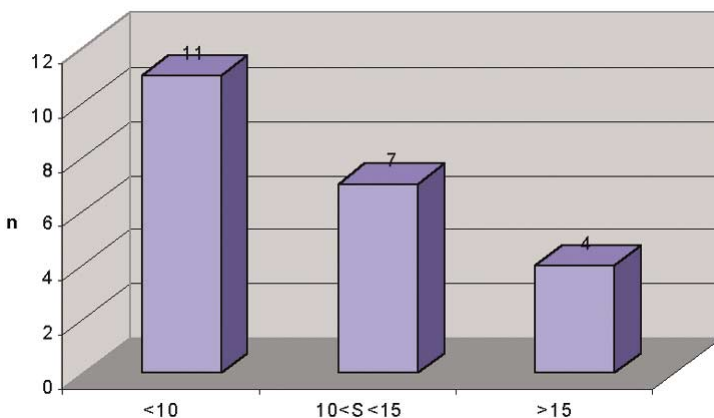
Results

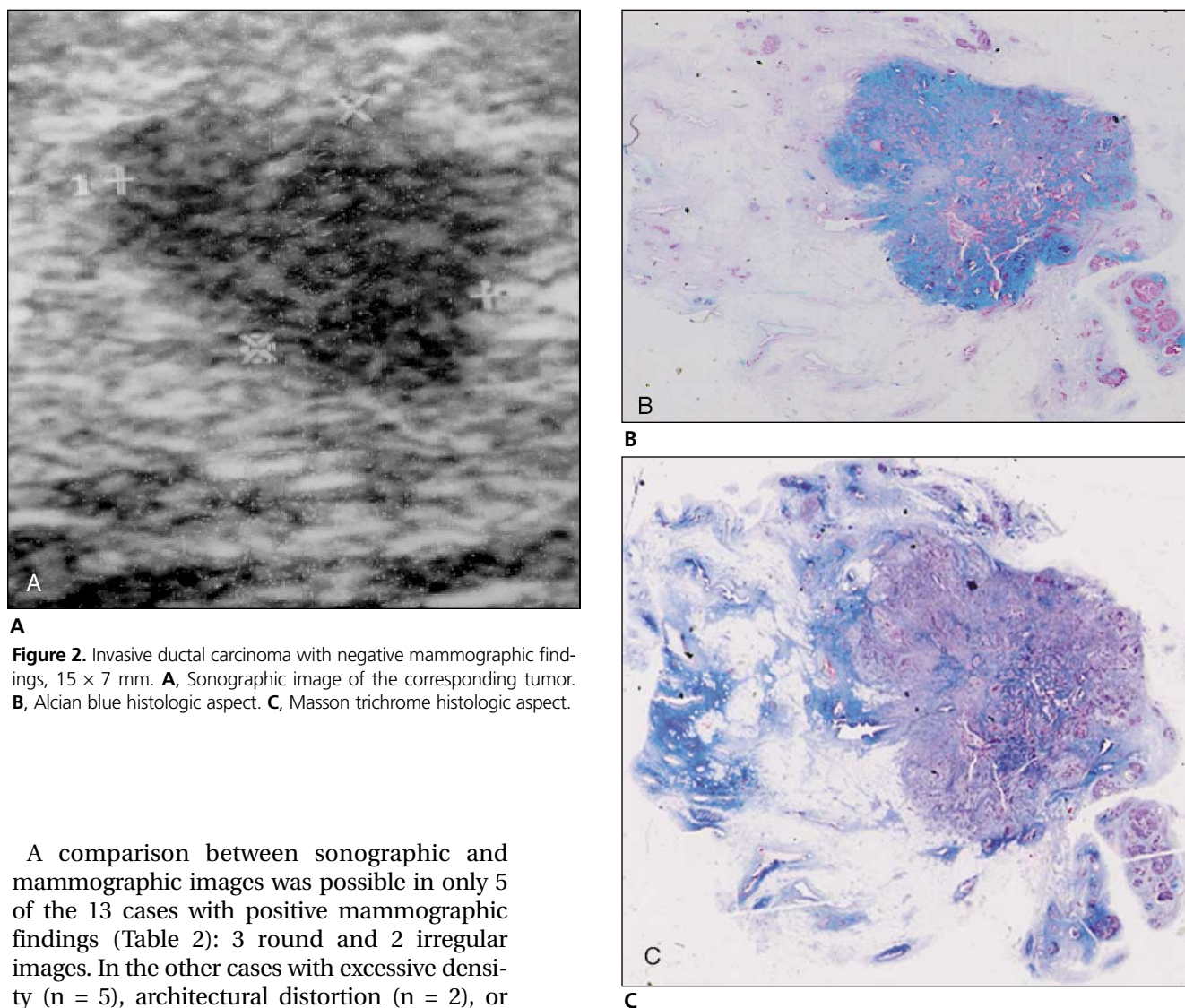
Except in 1 case in which the tumor seemed to have been ripped by forceps, the alcian blue distribution was nearly identical to the hypoechoic pattern. All the tumors were isoechoic (n = 9) or hypoechoic (n = 13) in relation to fat; none was hyperechoic. There was no difference between palpable and nonpalpable lesions. During the study's time frame, no invasive disease without a mass on sonography was depicted. The stained surface was slightly smaller than the hypoechoic zone in all cases (Figs. 2–7) with a very similar shape (Table 1): triangular (n = 2), round (n = 3), oval (n = 11), or irregular (n = 6).

The margins were indistinct and jagged (n = 12; Fig. 3) or indistinct and smooth (n = 10; Fig. 2) both on the alcian blue-stained sections and on the sonographic images. Posterior shadowing was present in 4 cases. In these cases, the posterior border was not shown, but the lateral and anterior borders were identical to those on the alcian blue-stained sections.

The tumors had a large amount of stroma, strongly stained by alcian blue, and were more or less not stained by trichrome (Fig. 7D) without adipose tissue. A heterogeneous pattern with scattered internal echoes was shown in almost all cases (n = 19). This pattern had been related to unequal distribution of alcian blue staining within the tumor, uptake predominating at the periphery. We were unable to make a quantified relationship between the intensity of the hypoechoic pattern and the intensity of the staining.

Figure 1. Size range of the lesions (millimeters).





A
Figure 2. Invasive ductal carcinoma with negative mammographic findings, 15 × 7 mm. **A**, Sonographic image of the corresponding tumor. **B**, Alcian blue histologic aspect. **C**, Masson trichrome histologic aspect.

A comparison between sonographic and mammographic images was possible in only 5 of the 13 cases with positive mammographic findings (Table 2): 3 round and 2 irregular images. In the other cases with excessive density ($n = 5$), architectural distortion ($n = 2$), or microcalcifications ($n = 1$), the contrast of the x-ray signal was insufficient to draw a precise shape. The 5 tumors were located in fatty breasts on mammography in patients older than 60 years. The shape of the tumor on the mammograms was identical to those on the scans and the alcian blue stains. However, in 2 cases with a major desmoplastic reaction (Fig. 7), the mammographic image was different and larger than the sonographic image or the alcian blue-stained section. Actually, the shape on the mammogram was identical to that of the Masson trichrome-stained section in which the tumor's stroma and desmoplastic peripheral tissue were highlighted.

In all cases except 3, the hyperechoic normal surrounding tissue was not stained by alcian blue was stained by trichrome and showed many

adipocytes and some normal glandular structure (Figs. 2–6). In the other 3 cases, the surrounding tissue was almost exclusively adipose tissue.

The fibroadenomas were hypoechoic with sharp and distinct margins (Fig. 8) and were stained strongly by Masson trichrome and slightly by alcian blue for hyaluronan. The internal echo pattern was homogeneous. The sonographic section of the umbilical cord confirmed the dye specificity: the hyaluronan-rich Wharton jelly was stained strongly by alcian blue and slightly by trichrome. Collagen fibers in vessels were stained strongly by trichrome. Stain intensities were comparable with those obtained in the tumor sections.

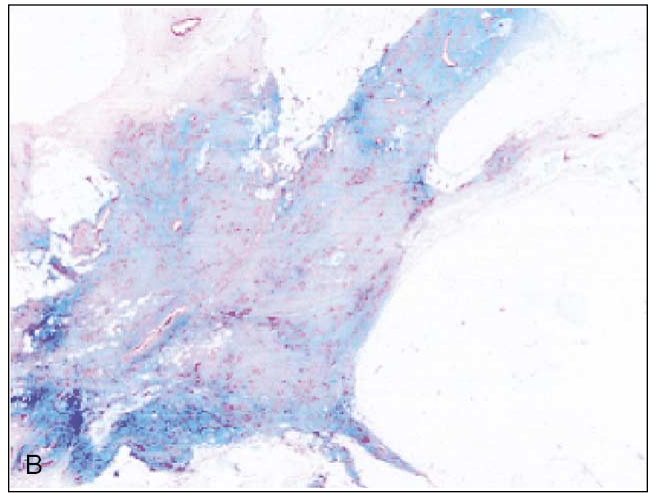
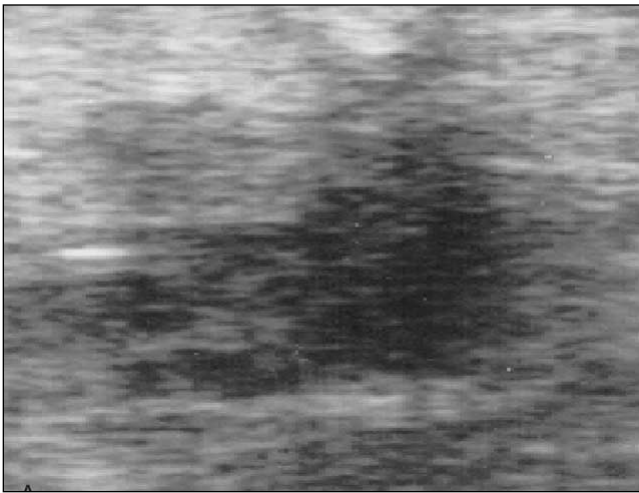


Figure 3. Invasive ductal carcinoma with negative mammographic findings; maximal tumor diameter, 15 mm. **A**, Sonographic image of the corresponding tumor. **B**, Alcian blue histologic aspect.

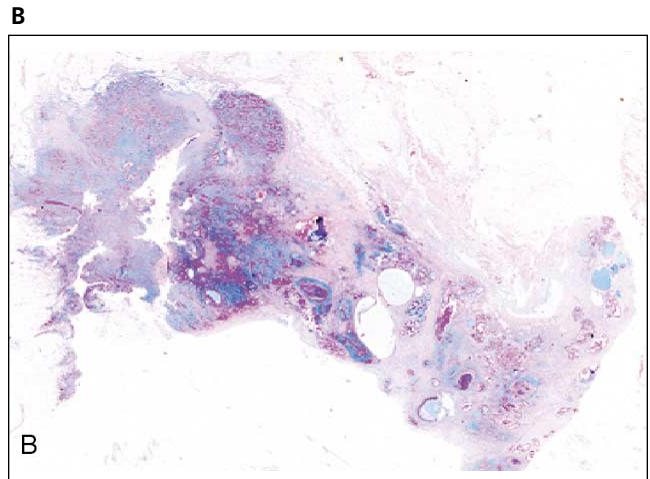
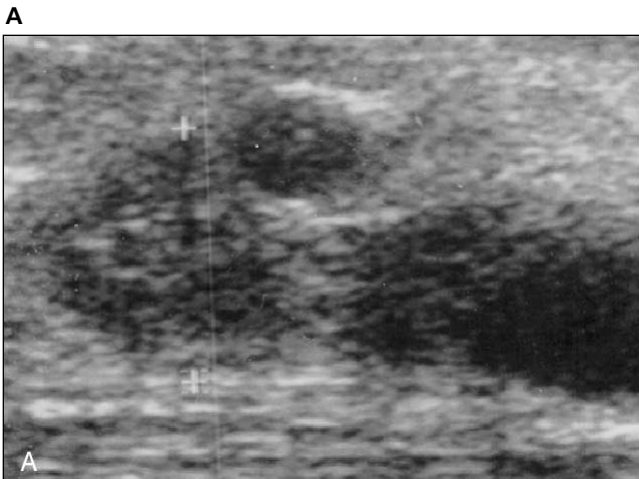
Discussion

Hyaluronan, a highly hydrated macromolecule, is a component of the extracellular matrix, which is involved in processes such as wound healing, tumor growth, and metastasis. It is expressed in both benign and malignant tumors³⁻⁵ and is restricted to stromal connective tissue. We have shown the relationship between the sonographic shape of the invasive breast tumor and the hyaluronan accumulation within the tumor's stroma. In almost all the tumors, the alcian blue tumor shape was roughly identical to the hypoechoic zone: the contours (angular or smooth),

the borders (sharp or indistinct), and the sizes were nearly identical on the sonographic image and on the histologic section. On a practical basis, the sonographic finding correlated with margins without any further extension in the surrounding tissue, which could underestimate the size of the specimen and should be removed to achieve clear margins at surgery.

Hyaluronan accumulation in the stroma could explain the hypoechogenicity, because it was the predominant component within the tumor and because the other main components (cells and collagen) have nearly the same acoustic impedance. Indeed, the cartilaginous portion of

Figure 4. Invasive ductal carcinoma with negative mammographic findings, 14 × 9 mm. **A**, Sonographic image of the corresponding tumor. **B**, Alcian blue histologic aspect.



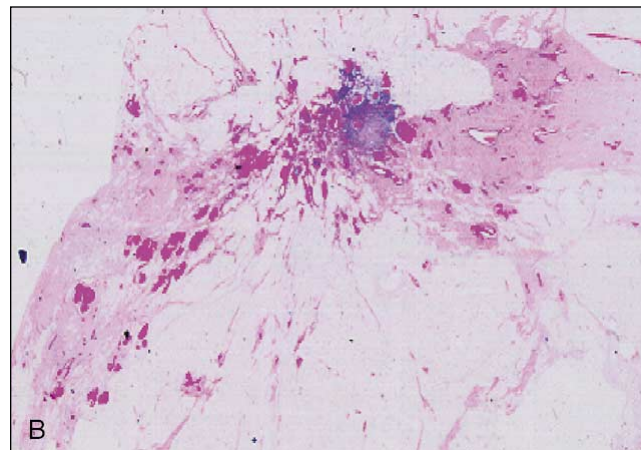
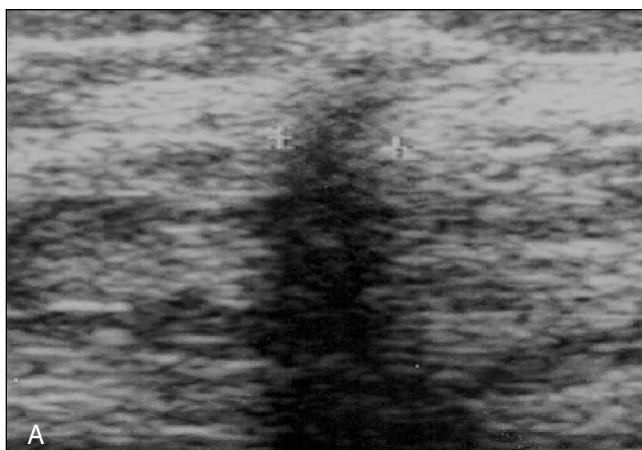


Figure 5. Invasive ductal carcinoma with negative mammographic findings; maximal tumor diameter, 6 mm. **A**, Sonographic image of the corresponding tumor. **B**, Alcian blue histologic aspect.

the ribs, which is made of the same extracellular matrix, is almost hypoechoic. The hyperechogenicity of the surrounding tissue was related to the presence of fat, which has an acoustic impedance very different from that of all other biological tissues,⁶ mixed with collagen and glandular structures.

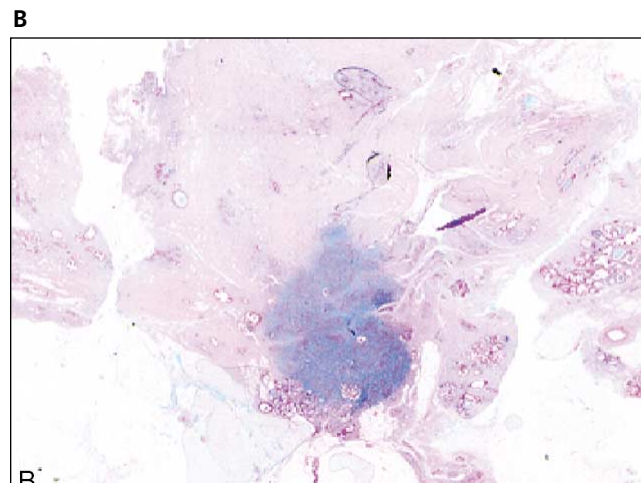
These findings cast new light on the sonographic image of invasive breast cancer. They also explain why sonography is so sensitive for

the detection of invasive breast cancer and why certain invasive tumors are not visible on mammograms.⁷⁻¹¹

Indeed, our findings indicate that breast sonography shows the extracellular modifications that support malignant cell proliferation. Our results concerned only invasive ductal carcinomas, but according to the histologic data,³ they could be generalized to other invasive breast cancer types, such as lobular, tubular,



Figure 6. Invasive ductal carcinoma with negative mammographic findings, 15 × 7 mm. **A**, Sonographic image of the corresponding tumor. **B**, Alcian blue histologic aspect.



mucinous, and medullary. Consequently, if no hypoechoic focal lesion can be detected on sonography, the likelihood of an invasive tumor is very low. This fact has been recently confirmed by Buchberger et al,¹¹ who showed that sonography missed only 1 of 95 invasive carcinomas. Furthermore, the 1 missed cancer had actually been visualized but as an undetermined hypoechoic mass. In another study,¹² sonography demonstrated all 8 invasive tumors among 100 mammographically detected clustered microcalcifications. All were solid masses with mild hypoechogenicity.

In contrast to this high performance of sonography, mammography reported in the study by

Buchberger et al¹¹ missed 35 invasive breast cancers. In a report by Kolb et al,¹³ 11 of 41 non-palpable cancers were shown only on sonography. Our findings can explain those results, because in dense breast, mammography is unable to distinguish the difference between the hydration of the dense surrounding tissue and the hydration of the hyaluronan-rich tumor. It is well established¹⁴ that radiologic density originates from a more or less hydrated tissue. Indeed, in one of our cases (Fig. 7), the radiologic density was identical to that of the trichrome-stained section (Fig. 7D), which stained the collagen within the tumor and within the surrounding desmoplastic reaction,

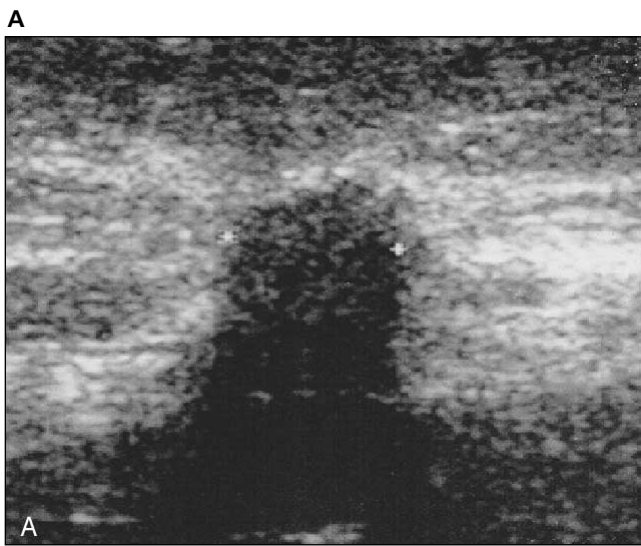


Figure 7. Invasive ductal carcinoma with positive mammographic findings, 15 × 9 mm. **A**, Sonographic image of the corresponding tumor. **B**, Alcian blue histologic aspect. **C**, Mammogram. **D**, Masson trichrome histologic aspect.

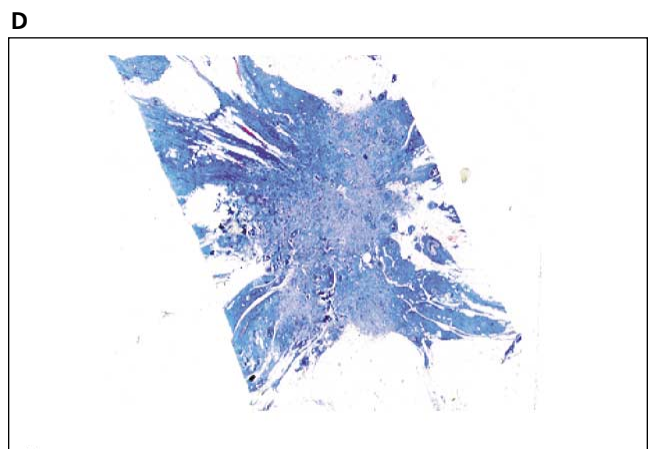
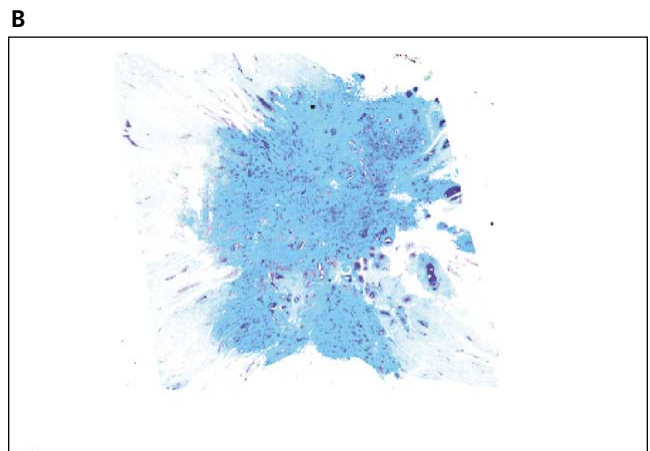
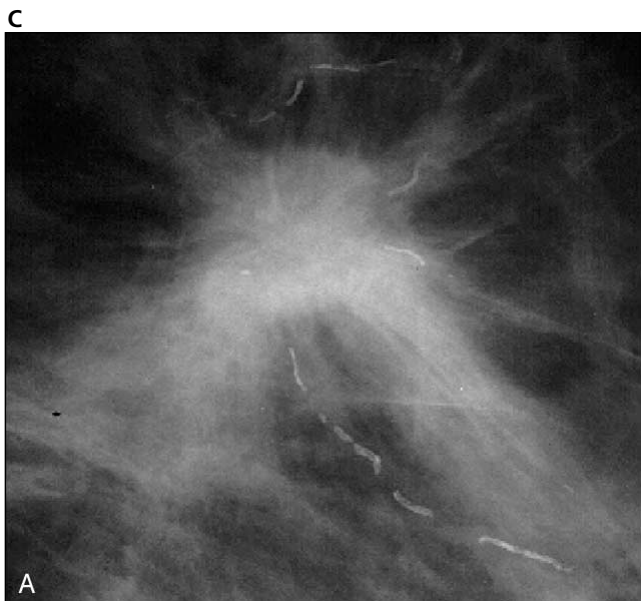


Table 1. Sonographic Features

Feature	n
Shape	
Triangular	2
Round	3
Oval	11
Irregular	6
Margins	
Indistinct and jagged	12
Indistinct and smooth	10
Echogenicity	
Isoechoic	9
Hypoechoic	13
Sound transmission	
Through-transmission	18
Posterior shadowing	4

although the hypoechoicity was related only to the alcian blue-stained section (only present within the tumor). Actually, in this case, the trichrome stain approximated more closely the mammographic size of the lesion than did the alcian blue stain.

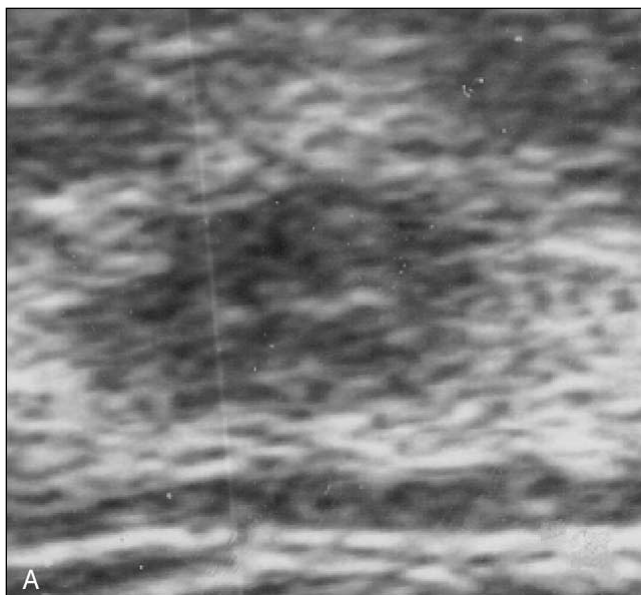
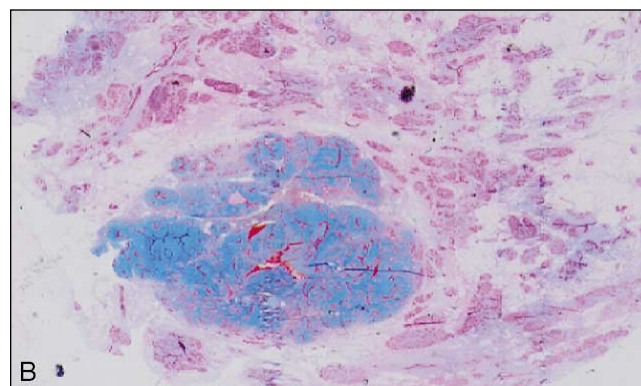
The large proportion of carcinomas not shown on radiology could have been attributable to a bias in this study, which was not related to patient selection but rather to the recruitment scheme. The patients included in this study were referred to a single practitioner working as a nonradiologist breast specialist, a specialty known to selectively recruit patients

Table 2. Mammographic Features

Feature	n
Round shape	3
Irregular shape	2
Excessive density	5
Architectural distortion	2
Microcalcifications	1
None	9

with such tumors. The major question is whether the paraffin block was cut in the exact same plane as the sonographic scan. We assumed that the greatest diameter of the histologic section was the same as that on the sonographic scan, but in some cases this may not have been true, which could have created an important bias. However, because the series was sequential, the strong relationship between the sections and the scans could not be related to a selection bias.

To our knowledge, there has been no previous report of this type of correlation between the sonographic morphology of infiltrating carcinoma and the accumulation of hyaluronan within the extracellular matrix. Teubner et al⁶ reported a study of the echo morphology and the histopathologic characteristics of breast carcinoma but came to a less precise conclusion. They demonstrated that the hypo-

A**Figure 8.** Fibroadenoma, 10 × 5 mm. **A**, Sonographic image of the corresponding tumor. **B**, Alcian blue histologic aspect.**B**

echogenicity was related to expanded fibro-hyalinosis in cases of invasive carcinomas. In 1979, Kobayashi¹⁵ showed a correlation between a retrotumoral shadow and the degree of desmoplasia, but we cannot support his conclusion. Although the tumor with desmoplasia in our study (Fig. 7A) was rich in collagen, the posterior shadow was related to the alcian blue area (Fig. 7B) and not to the trichrome stain (Fig. 7D). Additional studies are needed to understand this phenomenon, which could be linked to a calcification process of the extracellular matrix, because the negative charges of hyaluronan are able to bind cations of calcium. Among old patients, indeed, a process of calcification with shadowing occurs inside the cartilaginous portion of the ribs.

The relationship observed in our study cannot be taken as a real correlation because of the possible discrepancy between the histologic section and the sonographic scan. However, we have shown that the shape of the sonographic image of breast cancer was similar to the shape of its hyaluronan extracellular matrix. Further studies with quantitative analysis are needed. That could provide information on the degree of differentiation of the tumors, since intense hyaluronan expression is correlated to poor differentiation of carcinoma with statistical significance.³

References

1. Fornage BD, Toubas O, Morel M. Clinical, mammographic, and sonographic determination of preoperative breast cancer size. *Cancer* 1987; 60:765–771.
2. Yang WT, Lam WW, Cheung H, Suen M, King WW, Metreweli C. Sonographic, magnetic resonance imaging, and mammographic assessments of preoperative size of breast cancer. *J Ultrasound Med* 1997; 16:791–797.
3. Auvinen PK, Parkkinen JJ, Johansson RT, et al. Expression of hyaluronan in benign and malignant breast lesions. *Int J Cancer* 1997; 74:477–481.
4. De la Torre M, Wells AF, Bergh J, Lindgren A. Localization of hyaluronan in normal breast tissue, radial scar, and tubular breast carcinoma. *Hum Pathol* 1993; 24:1294–1297.
5. Bertrand P, Girard N, Delpech B, Duval C, d'Anjou J, Dauce JP. Hyaluronan (hyaluronic acid) and hyaluronectin in the extracellular matrix of human breast carcinomas: comparison between invasive and non-invasive areas. *Int J Cancer* 1992; 52:1–6.
6. Teubner J, Bohrer M, van Kaick G, Georgi M. Correlation between histopathology and echomorphology in breast cancer. In: Madjar H, Teubner J, Hackelöer B (eds). *Breast Ultrasound Update*. Basel, Switzerland: Karger; 1994:63–74.
7. Gordon PB, Goldenberg SL, Chan NH. Solid breast lesions: diagnosis with US-guided fine needle aspiration biopsy. *Radiology* 1993; 189:573–580.
8. Rotten D, Levaillant JM, Le Floch JP, Constancis E, Andre JM. Mass screening for breast cancer with sonomammography: a prospective study. *Eur J Obstet Gynecol Reprod Biol* 1988; 28:257–267.
9. Stavros AT, Thickman D, Rapp CI, Dennis MA, Parker SH, Sisney GA. Solid breast nodules: use of sonography to distinguish between benign and malignant lesions. *Radiology* 1995; 196:123–134.
10. Fornage BD, Sneige N, Faroux MJ, Andry E. Sonographic appearance and ultrasound-guided fine-needle aspiration biopsy of breast carcinomas smaller than 1 cm³. *J Ultrasound Med* 1990; 9:559–568.
11. Buchberger W, Niehoff A, Obrist P, DeKoekkoek-Doll P, Dunser M. Clinically and mammographically occult breast lesions: detection and classification with high-resolution sonography. *Semin Ultrasound CT MR* 2000; 21:325–336.
12. Moon WK, Im JG, Koh YH, Noh DY, Park IA. US of mammographically detected clustered microcalcifications. *Radiology* 2000; 217:849–854.
13. Kolb TM, Lichy J, Newhouse JH. Occult cancer in women with dense breasts: detection with screening US-diagnostic yield and tumor characteristics. *Radiology* 1998; 207:191–199.
14. Lamarque JL, Rodiere MJ, Fontaine A, et al. Anatomical and histological approach to the radiographic appearance of the breast. *J Radiol Electrol Med Nucl* 1976; 57:753–766.
15. Kobayashi T. Diagnostic ultrasound in breast cancer: analysis of retrotumorous echo patterns correlated with sonic attenuation by cancerous connective tissue. *J Clin Ultrasound* 1979; 7:471–479.